SURFACE AND INTERFACE ANALYSIS
Surf. Interface Anal. 2002; **33**: 945–949
Published online in Wiley InterScience (www.interscience.wiley.com). DOI: 10.1002/sia.1475

SIA

Ammonia adsorption on Zr(0001): effect of electron bombardment on hydrogen production

N. Stojilovic, Y. C. Kang and R. D. Ramsier*

Departments of Physics, Chemistry, and Chemical Engineering, The University of Akron, Akron, OH 44325-4001, USA

Received 10 July 2002; Revised 15 August 2002; Accepted 28 August 2002

With the ultimate goal of modifying the surface chemistry of zirconium, we present a temperature-programmed desorption (TPD) study of ammonia adsorbed on Zr(0001) followed by soft electron bombardment. The TPD data indicate that water accompanies the thermal desorption of ammonia near 730 K, which is a result of the mixing of oxygen atoms from the subsurface region with ammonia dissociation products. Nitrogen is left at the surface following TPD and can be removed only by repeated sputtering cycles. These thermal effects occur with or without electronic excitation. Electron bombardment does, however, result in the desorption of hydrogen gas in TPD near 310 K, indicating the formation of new hydrogenic species at the surface via electronic excitation. The electron-induced cross-sections for the production of these species are determined to be in the 1–5($\times 10^{-18}$) cm^2 range. Copyright © 2002 John Wiley & Sons, Ltd.

KEYWORDS: ammonia; zirconium; electron bombardment; TPD

INTRODUCTION

Ammonia adsorption on surfaces has been the subject of many investigations, and those that use electron bombardment for activating non-thermal processes are usually focused on the formation of nitride layers. Recently, we reported a study of the thermal behavior of the NH_3/Zr(0001) system using temperature-programmed desorption (TPD) techniques.[1] In this work the desorption temperatures, peak profiles and yields of ammonia are all found to be strongly dependent on adsorption temperature. Desorption of water following ammonia adsorption is also detected in TPD, indicating an involvement of oxygen from the zirconium subsurface region. The rich kinetic behavior that this system exhibits is worth pursuing in greater detail, and the present paper concerns the use of soft electron bombardment to modify its surface chemistry.

Electronic excitation of surface species is induced with an electron beam (485 eV) following ammonia adsorption. Although no nitride layers are observed by AES, hydrogen desorption at 310 K is detected in TPD as a direct consequence of electron bombardment. We vary the electron fluence while keeping the ammonia exposure approximately constant, and also vary the adsorption temperature and ammonia exposure while keeping the electron fluence constant. We observe that the effect of electron bombardment in all cases is the production of a low-temperature hydrogen desorption state in TPD. We determine that the cross-sections for production of these low temperature hydrogenic species are in the 1–5($\times 10^{-18}$) cm^2 range. Within experimental uncertainties there are no electron-induced effects on the amount of nitrogen left at the surface after TPD, on the TPD yields of ammonia and water or on the formation of superstructure low-energy electron diffraction (LEED) patterns. We thus demonstrate that electronic excitation can be used to modify selectively the low-temperature kinetics of the NH_3/Zr(0001) system without significantly perturbing its high-temperature behavior.

*Correspondence to: R. D. Ramsier, Departments of Physics, Chemistry and Chemical Engineering, The University of Akron, Akron, OH 44325-4001, USA. E-mail: rex@uakron.edu
Contract/grant sponsor: Donors of the American Chemical Society Petroleum Research Fund.
Contract/grant sponsor: Research Corporation.

EXPERIMENTAL

Detailed description of the stainless-steel ultrahigh vacuum (UHV) system used in this work can be found elsewhere.[2] Briefly, the system is pumped by turbomolecular, ion getter and titanium sublimation pumps and operates at a base pressure of 3×10^{-10} Torr for the experiments discussed here. The Zr(0001) sample is a cylindrical disk with a radius of 3 mm and a thickness of 1 mm. One side of the sample is polished to 0.03 μm with an accuracy of orientation better than 1°. Two type-E thermocouples spot-welded to the sides of the sample complete a temperature-controlled feedback loop. Tantalum wires, also spot-welded to the sides of the sample, provide d.c. heating. Cooling is provided by a copper braid connected to a liquid-nitrogen cold finger.[3] For most of the data presented in this work, ammonia adsorption is performed with the sample temperature near 155 K.

The sample surface is cleaned by cycles of argon ion sputtering (2 keV, 2 μA cm^{-2}) followed by annealing to 840 K for 2 min until sharp (1 × 1) reverse-view LEED (65 eV, 2 μA cm^{-2}) patterns are observed. Retarding-field

AES (3 keV, 15 μA cm^{-2}) indicates the presence of small amounts of oxygen and carbon at the surface due to gettering by the reactive zirconium substrate, similar to what is observed by others.[4] We find AES ratios after sputtering and annealing to be approximately C KLL/Zr MNN = 0.21, O KLL/Zr MNN = 0.15 and Zr MNN/Zr MNV = 1.1, where MNN and MNV signify the Zr transitions near 94 and 148 eV, respectively. It is known that our cleaning procedure leaves some carbon and oxygen at the surface,[3,4] but also that keeping the annealing temperature below 900 K avoids unwanted segregation of sulfur to the surface. The latter AES ratio does not indicate significant sulfur segregation because the S LMM feature at 152 eV overlaps with the Zr MNV transition, making the Zr MNN/Zr MNV ratio much smaller.[4] The influence of sulfur on our AES spectra is an issue that we have investigated and found that with the adsorption of SO_2 and annealing we could change this ratio to ~0.2 (not shown). Thus we are convinced that, although our annealed surface contains some oxygen and carbon, we do not have significant sulfur concentration at the surface in the experiments reported here.

The sample is exposed to ammonia (99.99% purity) by backfilling the chamber through a precision leak valve connected to a stainless-steel gas-handling system. Electron bombardment of the entire sample surface is performed with 485 eV electrons from a well-regulated flood gun. The TPD data are collected with a quadrupole mass spectrometer in line-of-sight geometry at a temperature ramp of 1.7 K s^{-1}. The LEED and AES data are collected with the sample near 155 K after stepwise annealing with the same temperature ramp.

RESULTS AND DISCUSSION

The surface chemistry of zirconium is complex because it dissociatively adsorbs gases and readily absorbs their dissociation products. Early work clearly indicates that the dissociative chemisorption of small molecules on Zr leads to surface–subsurface diffusion and complicated kinetics.[5] The presence of oxygen near the surface induces the outward segregation of hydrogen,[6,7] and observations implying that nitrogen preferentially occupies subsurface sites[1,5,8] have been supported by theoretical calculations.[9] Models of adsorption and desorption kinetics in the presence of surface–subsurface exchange have been proposed,[10,11] and are complicated by the possibility of co-adsorbate interactions and surface coverage effects.

Nevertheless, we have managed to learn a considerable amount about this interesting materials system. For the case of ammonia adsorption on Zr(0001) we find that the subsequent thermal behavior strongly depends on the adsorption temperature.[1] Depending on adsorption conditions, water and ammonia desorb in broad TPD features extending across the 500–800 K range. Nitrogen remaining near the surface forms no superstructure LEED patterns except for an enhanced brightness of the (1 × 1) spots after annealing. These results are again verified in the present study, and we see no significant changes in our AES and LEED data due to soft electron bombardment. In particular, we see no evidence for shifts of the Zr MNV features that would indicate the formation of oxide[12] or nitride[13] layers. This is different from the behavior seen for ammonia adsorbed on the surfaces of semiconductors,[14,15] where electronic excitation has been shown to enhance surface nitride formation. Because there is little change in our AES and LEED data due to electron bombardment, we will focus on the TPD results.

Figure 1 presents a set of 17 amu TPD spectra from Zr(0001) following ammonia adsorption and electron bombardment. These 17 amu spectra represent a combination of NH_3^+ and OH^+ signals from ammonia and water, respectively, which desorb together as verified by also monitoring the 18, 16, 15 and 14 amu signals. The broad desorption features develop with ammonia exposure similar to those without electron bombardment,[1] with peak desorption temperatures dependent on the adsorption conditions. Because our interpretation of these desorption features involves migration and mixing of subsurface oxygen with adsorbed-absorbed nitrogen and hydrogen, it is reasonable that electronic excitation does little to affect peak profiles or temperatures. Adsorbates present on Zr(0001) at low temperature may differ from those on other metal surfaces,[16–18] where electron bombardment clearly damages some species and alters the subsequent ammonia TPD spectra.[18] The reactive nature of Zr may account for such differences, as more dissociation during adsorption is expected in the present situation.

This view is consistent with the data of Fig. 2, which indicate no significant difference in the integrated yields of ammonia in TPD due to electron bombardment. The slow

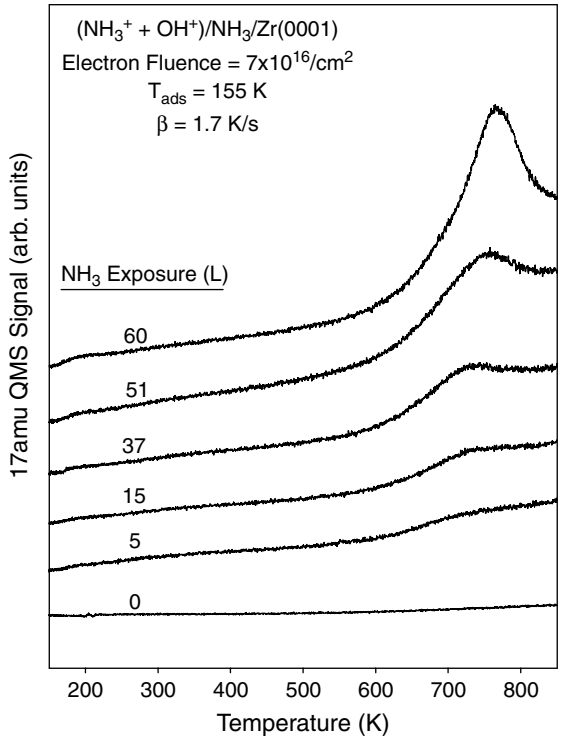

Figure 1. The $NH_3^+ + OH^+$ TPD spectra following 155 K ammonia adsorption on Zr(0001) at a fixed fluence of 485 eV electrons.

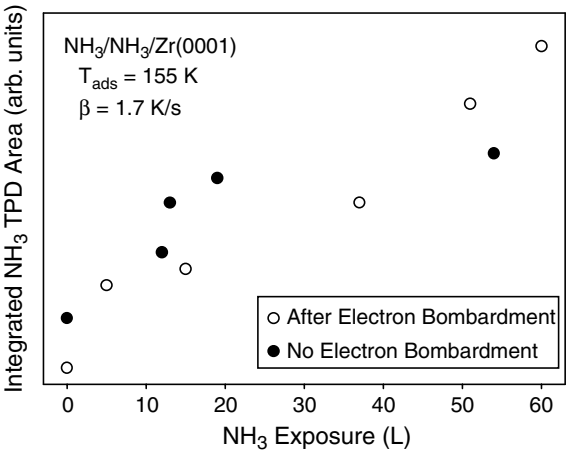

Figure 2. Integrated TPD yield of ammonia from Zr(0001), indicating that 485 eV electron bombardment (fluence = 7×10^{16} cm^{-2}) has very little effect. Electron exposure such as this takes only 5 min, during which time background contamination is not significant.

pumping speed of ammonia and the sloping backgrounds of the ammonia and water TPD spectra make the baseline fitting for integration and exposure calculations difficult. The uncertainty in the yield data of Fig. 2 is represented by the two data points at zero ammonia exposure. It should be noted that these data have been corrected by subtracting out the OH^+ contribution determined from the known cracking pattern of water and the 18 amu TPD spectra. The TPD spectra with and without electron bombardment do not indicate the production of N_2, O_2, NO or other possible oxygen- or nitrogen-containing species except water and ammonia. In the absence of electron bombardment, there is a very small water/ammonia desorption feature near 175 K following 155 K adsorption. The species responsible for this appear to be sensitive to electron bombardment because we see no low-temperature desorption in Fig. 1.

However, there is a much more interesting effect that can be seen in the H_2^+ TPD spectra. Figure 3 shows how hydrogen TPD data from NH_3/Zr(0001) depend on electron fluence. It is clear that the production of this low-temperature hydrogen is a result of electronic excitation. In addition to the hyperthermal production of a new desorption state, the most interesting observation is that the desorption temperature of this feature does not shift with adsorption temperature or ammonia exposure. On the other hand, water and ammonia TPD features strongly depend on adsorption conditions.[1] Lower adsorption temperatures result in higher desorption temperatures and smaller TPD yields. Because our mechanistic understanding of the recombinative desorption of NH_3 and H_2O involves surface–subsurface diffusion, we are led to the conclusion that the H_2 evolution that we report in this paper results from some form of surface-bound hydrogen that is not present in the absence of electron bombardment.

The propensity for dissociative adsorption and subsurface diffusion obviously depends on the adsorption temperature. The deeper into the subsurface the species dissolve, the less likely they are to return to the surface during TPD and recombinatively desorb. This is why our ammonia and water

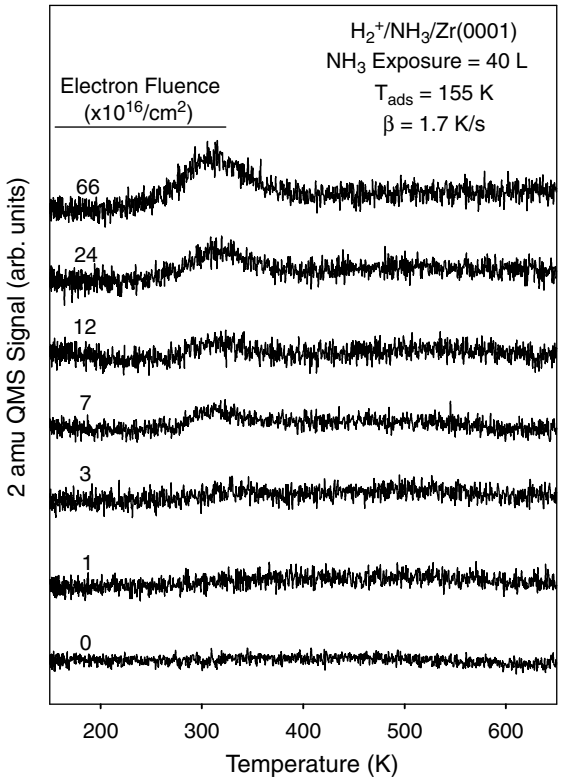

Figure 3. Hydrogen TPD spectra following 155 K ammonia adsorption on Zr(0001) and electron bombardment. The production of H_2^+ depends on the fluence of 485 eV electrons. We have verified that data such as these do not depend sensitively on ammonia exposure, and for this data set the ammonia exposures are kept at ~40 L.

TPD spectra are broad and adsorption temperature dependent—they indicate mass transport from beneath the surface. However, this is not the case with the H_2 desorption feature induced by electron bombardment. Because the baseline is well-defined in the hydrogen TPD spectra, we can calculate the integrated area of the 310 K TPD features with high accuracy and extract cross-sections for production of the species responsible for their appearance. These data are shown in Fig. 4 for two adsorption temperatures; 180 K and 155 K. The exponential fits yield cross-section values of 4.4 ± 0.3 and 1.7 ± 0.7, respectively, in the units of 10^{-18} cm^2. These values are what one would expect for electron-induced surface processes in general,[19] and are quantitatively lower than those recently reported for the total cross-sections for ammonia dissociation on other less reactive metals.[17,18] Because we determine cross-sections for the production of species that liberate hydrogen during TPD, and not for all electron-stimulated processes such as ion and neutral desorption, we expect our values to be lower than those found in these other studies. It should be noted that our 180 K experiments avoid the species responsible for the small 175 K desorption feature mentioned in the discussion of Fig. 1. However, 180 K adsorption yields a cross-section for hydrogen production that is essentially the same as that for 155 K adsorption.

The nature of this electronically induced surface chemistry is unknown at present. Most probably, ammonia dissociates thermally upon adsorption under the present

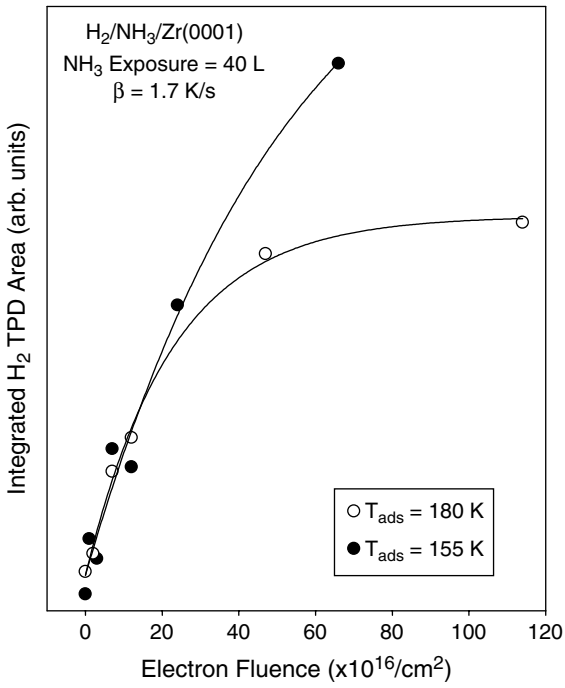

Figure 4. Integrated TPD yields from the low-temperature hydrogen state as a function of electron fluence for two different ammonia adsorption temperatures. The exponential fits yield cross-sections in the 1–5($\times 10^{-18}$) cm^2 range.

conditions, yielding adsorbed (a) NH_x and hydrogen species, where $x < 3$. One logical interpretation of our data is that upon adsorption of ammonia from the gas phase (g), H(a) diffuses into the subsurface (s) region to produce H(s) in the following manner

$$NH_3(g) \rightarrow NH_2(a) + H(a) \rightarrow NH_2(a) + H(s) \qquad (1)$$

Without electron bombardment, TPD heating results in

$$2NH_2(a) + 2H(s) + O(s) \rightarrow 2N(a) + 6H(s)$$
$$+ O(s) \rightarrow NH_3(g) + H_2O(g) + N(a) + H(s) \qquad (2)$$

which disproportionately leaves nitrogen behind, as we observe by AES and infer from LEED. In fact, our TPD yields of water and ammonia are comparable, with water even dominating under some conditions.

With electron (e) bombardment, another channel is possible before TPD

$$NH_2(a) + e \rightarrow NH(a) + H(a) \rightarrow NH(a) + H(s) \qquad (3)$$

which, upon heating, leads to the low-temperature reaction

$$2NH(a) \rightarrow H_2(g) + 2N(a\text{–}s) \qquad (4)$$

where the remaining nitrogen stays on the surface or migrates to the subsurface region.

Of course the scenario proposed above is only one possibility. We know that oxygen and carbon are present in small quantities on the surface before ammonia exposure. The backfilling process and active gettering by zirconium may lead to an increase in surface impurities even under UHV conditions. Because we do not see significant CO or CO_2 desorption in TPD, we assume that surface carbon does not contribute to any great extent in the thermal or electron-induced chemistry of this surface under the present conditions. However, there is a strong indication of oxygen participation in the production of water during TPD.

We observe an increase in the oxygen AES signal after ammonia adsorption. This is either due to adsorption of oxygen-containing impurities such as water, or to exchange of surface nitrogen from dissociatively adsorbed ammonia with subsurface oxygen. Surface oxygen is known to induce the outward segregation of hydrogen and trap it near the surface, either as hydroxyl species or some stabilized form of surface hydride. Thus we must consider the possibility that species such as OH(a) or ZrH(a) might also be contributing to the low-temperature hydrogen production, similar to the role of NH(a) that we propose in Eqn. (4). We have already shown that charging Zr(0001) with isotopic oxygen before TPD reveals the mixing of surface and subsurface species.[20] Theoretical predictions of the binding energies of oxygen and nitrogen in the subsurface region of Zr(0001) also indicate that nitrogen is more stable than oxygen between the first and second Zr layers.[9] These previous results indicate that the increase we see in the oxygen AES signal after ammonia adsorption may not be due to surface impurities but to the complicated surface–subsurface kinetics that this material exhibits.

CONCLUSIONS

We demonstrate that low-energy electron bombardment following ammonia adsorption can be used to modify the thermal evolution of hydrogen from Zr(0001). We determine electron-induced cross-sections for the production of hydrogen gas and propose explanations for its origin. The reactive nature of Zr makes the influence of electron irradiation less pronounced than in other systems, but at the same time gives us the ability to perturb finely the resulting surface chemistry. Studies such as this may help us to understand the environmentally assisted degradation of this class of materials during service in radiation environments, as well as to improve our knowledge of electronically induced surface chemistry in general.

Acknowledgements

Acknowledgment is made to the Donors of the American Chemical Society Petroleum Research Fund for partial support of this research. Partial support of our efforts by Research Corporation is also acknowledged.

REFERENCES

1. Kang YC, Ramsier RD. *Vacuum* 2002; **64**: 113.
2. Kang YC, Milovancev MM, Clauss DA, Lange MA, Ramsier RD. *J. Nucl. Mater*. 2000; **281**: 57.
3. Kang YC, Ramsier RD. *J. Nucl. Mater*. 2002; **303**: 125.
4. Ojima K, Ueda K. *Appl. Surf. Sci*. 2000; **165**: 141.
5. Foord JS, Goddard PJ, Lambert RM. *Surf. Sci*. 1980; **94**: 339.
6. Asbury DA, Hoflund GB, Peterson WJ, Gilbert RE, Outlaw RA. *Surf. Sci*. 1987; **185**: 213.
7. Ojima K, Ueda K. *Appl. Surf. Sci*. 2000; **165**: 149.

8. Wong PC, Mitchell KAR. *Surf. Sci*. 1987; **187**: L599.
9. Yamamoto M, Kurahashi M, Chan CT, Ho KM, Naito S. *Surf. Sci*. 1997; **387**: 300.
10. Li B, Zhang C-S, Zhdanov VP, Norton PR. *Surf. Sci.* 1995; **322**: 373.
11. Kovar M, Griffiths K, Kasza RV, Shapter JG, Norton PR. *J. Chem. Phys*. 1997; **106**: 4797.
12. Nishino Y, Krauss AR, Lin Y, Gruen DM. *J. Nucl. Mater*. 1996; **228**: 346.
13. Kurahashi M, Yamamoto M, Mabuchi M, Naito S. *J. Vac. Sci. Technol. A* 1997; **15**: 2548.
14. Bater C, Sanders M, Craig JH Jr. *Surf. Interface Anal*. 2000; **29**: 208.
15. Bater C, Sanders M, Craig JH Jr. *Surf. Sci*. 2000; **451**: 226.
16. Chrysostomou D, Flowers J, Zaera F. *Surf. Sci*. 1999; **439**: 34.
17. Mocuta D, Ahner J, Yates JT Jr. *Surf. Sci*. 1997; **383**: 299.
18. Bater C, Campbell JH, Craig JH Jr. *Surf. Interface Anal*. 1998; **26**: 97.
19. Ramsier RD, Yates JT Jr. *Surf. Sci. Rep*. 1991; **12**: 243.
20. Kang YC, Ramsier RD. *Appl. Surf. Sci*. 2002; **195**: 196.